EXPLORING THE MECHANICAL PERFORMANCE AND MATERIAL STRUCTURES OF INTEGRATED ELECTRICAL CIRCUITS WITHIN SOLID STATE METAL ADDITIVE MANUFACTURING MATRICES

J. Li*, T. Monaghan, A. Bournias-Varotsis, S. Masurtschak, R. J. Friel, and R. A. Harris

Wolfson School of Mechanical and Manufacturing Engineering, Loughborough University, Loughborough, Leicestershire, LE11 3TU, UK

REVIEWED

Abstract

Ultrasonic Additive Manufacturing (UAM) enables the integration of a wide variety of components into solid metal matrices due to a high degree of metal plastic flow at low matrix bulk temperatures. This phenomenon allows the fabrication of previously unobtainable novel engineered metal matrix components.

The aim of this paper was to investigate the compatibility of electronic materials with UAM, thus exploring an entirely new realm of multifunctional components by integration of electrical structures within dense metal components processed in the solid-state. Three different dielectric materials were successfully embedded into UAM fabricated metal-matrices with, research derived, optimal processing parameters.

The effect of dielectric material hardness on the final metal matrix mechanical strength after UAM processing was investigated systematically via mechanical peel testing and microscopy. The research resulted in a quantification of the role of material hardness on final UAM sample mechanical performance, which is of great interest for future industrial applications.

1. Introduction

Ultrasonic Additive Manufacturing (UAM) utilizes ultrasonic vibrations to weld metal foils layer by layer, and then periodically applies Computer Numerical Control (CNC) machining to produce a 3D solid structure [1]. Fig. 1 shows a schematic of the UAM weld system. This weld system uses a textured sonotrode to ultrasonically oscillate and apply a compressive normal force to the metal foils to be welded. This oscillation causes friction and deformation at the interface between the upper foil and the substrate which breaks metal surface oxide films and results in a clean, intimate surface contact. Metallurgical bonding at the interface is achieved in the solid state.

Due to a high degree of metal plastic flow at a low processing temperature, UAM enables the integration of electrical components into solid metal matrices in a layer by layer fashion. Several electrical components, such as optical fibre sensor [2], pre-packaged temperature sensor [3], and direct-written circuitries [4], have previously been encased into metal matrices via UAM. The potential for embedding freeform electrical components and circuitries within dense metal components processed by UAM presents many interesting opportunities for a

range of technology sectors from aerospace to civil engineering. The successful integration of freeform circuitry and sensors into solid metal matrices would permit the manufacture of novel multifunctional complex structures that have been previously unobtainable.
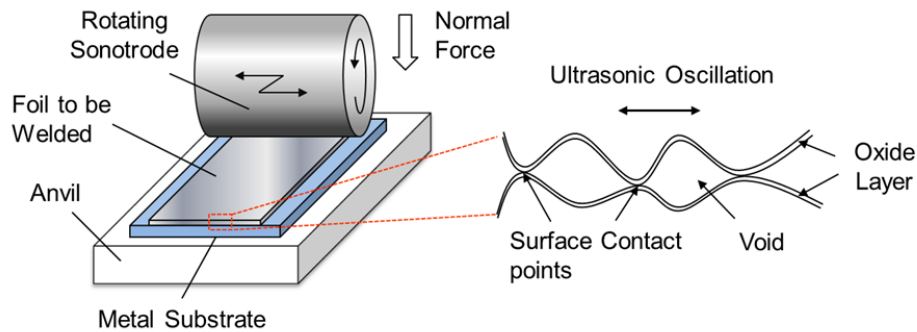

Fig. 1: Schematic of the Ultrasonic Additive Manufacturing (UAM) weld system.

To realise these new structures a hybrid multi manufacturing systems approach was need. The materials and capabilities of the necessary manufacturing systems need to be investigated in unison to identify the key factors. This paper documents an investigation into the compatibility of printed electronic materials with the UAM process.

2. Methodology

2.1 Sample Preparation

A 5 mm thick and 30 mm wide aluminium (Al) 1050 H14 plate was used as a base plate for the UAM process, and two Al 3003 H18 foils with the thickness and width of 100 µm and 25.4 mm respectively were sequentially welded onto the base plate to create the initial metal matrix (Fig. 2(a)). The UAM Alpha 2 system with parameters of 1600 N normal force, 25 µm sonotrode amplitude, and 20 mm/s welding speed, respectively, was used. These parameters were obtained via systematic tests and prior studies focused on the UAM of 3003 H18 aluminium [5-7] to produce high strength Al-Al welding.
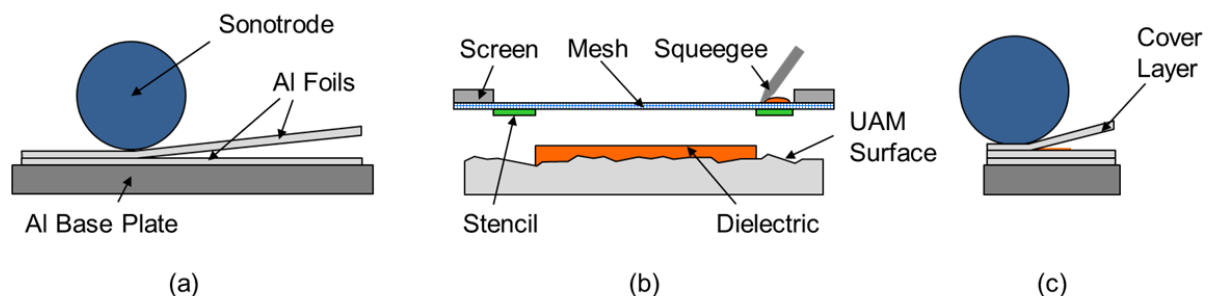

Fig. 2: The sample preparation method that combines screen printing electrical materials on to UAM surfaces and subsequent UAM encapsulation into solid metal matrix.

Three dielectric inks, LuxPrint® 8153 from DuPont™, 520 Series Soldermask made by Technic, and Imagecure® AQ XV501T-4 of Sunchemical® were employed in the experiments and screen printed on the UAM deposited Al substrate by DEK 265 horizon printer (Fig. 2(b)). After that, all three inks were cured/solidified thermally as per the manufacturer's instructions [8-10]. The final cure sample dimensions are 38 mm long, 3 mm wide, and around 45 µm thick (Fig. 3). Thin and small area dielectric film may be desirable for embedding via UAM process. However, in future work dielectrics will be used to encapsulate printed electrical conductive structures to build electrical devices, so dielectric films with the similar dimensions of finished electrical devices were fabricated and tested in this paper.
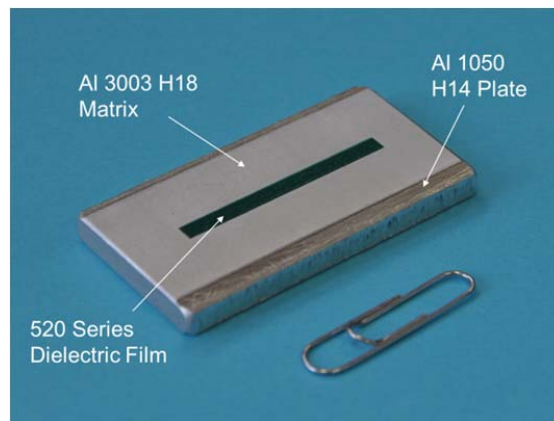

Fig. 3: 520 Series dielectric film deposited on UAM processed Al substrate.

The screen printed dielectric layers were then encased by ultrasonically welding another Al 3003 H18 foil on the substrate (Fig. 2(c)). Two combinations of control parameters with different UAM processing energy were applied to embed the electronics: a higher UAM energy combination was used to fabricate one set of metal matrices: 1600 N normal force, 25 µm sonotrode amplitude, and 20 mm/s welding speed; and a lower UAM energy set was 800 N normal force, 15 µm sonotrode amplitude, and 10 mm/s welding speed. The low energy combination was obtained by systematically embedding three dielectric films until there was no fracture caused by UAM in Al cover foils.

2.2 Testing Methods

Vickers Micro-Hardness

The hardness of the dielectric material was thought to be of importance for embedding as the material would need to be sufficiently hard to resist excessive deformation during the embedding process but also ductile enough to prevent cracking and disintegration when exposed to the cyclic loading of the UAM process. Hardness of dielectric materials was not found to be published or common knowledge. In order to establish the hardness of the printed dielectric materials a Mitutoyo HM-124 micro-Vickers hardness testing machine was used to measure the hardness of the three cured dielectric materials (Fig. 4 (a)). Indentations were performed under the load control mode that increased the load to a pre-set value and held for a certain time to reduce the influence of creep (Fig. 4(b)). The maximum load applied to all three dielectrics was

0.05 kg and the load duration time was set to be 10 s. The two diagonals of the indentation left in the surface of the material after removal of the load were measured using a microscope (Fig. 4(c)). The area of the sloping surface of the indentation was calculated. The Vickers hardness is the quotient obtained by dividing the kilogram-force load by the square millimetre area of indentation.
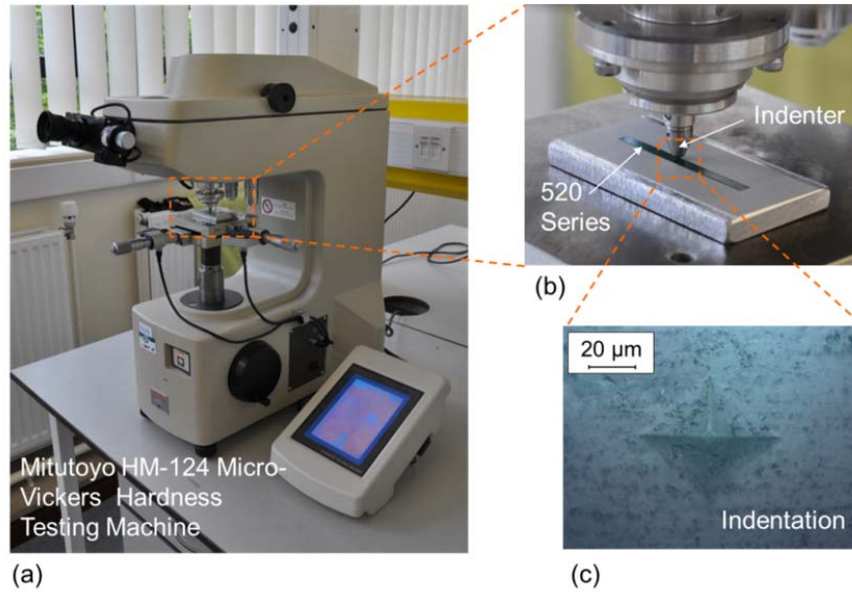

Fig. 4: (a) The photo of Mitutoyo HM-124 micro-Vickers hardness testing machine; (b) micro-Vickers hardness test on 520 Series dielectric film; and (c) an indentation made on 520 Series dielectric film under the load of 0.05 kg.

Mechanical Peel Testing

Peeling tests were performed in accordance with BS EN 2243-2 2005. For each dielectric embedded with both the higher and lower UAM settings three samples were peeled and the average peel load was calculated. Samples with no embedded dielectric were also fabricated using both lower and higher parameter combinations and tested in the same way as the dielectric containing samples. By comparing the peeling loads for the samples with and without dielectric films any potential mechanical strength change could be clearly revealed.

Optical Microscopy

Embedded samples were cross-sectioned and investigated via optical microscopy. Linear Weld Density (LWD) was used to describe the percentage of bonded area along the weld interface, the proportion of encased dielectric area to the total embedment interface and is expressed as:

$$LWD(\%) = \frac{L_b}{L_i} \times 100 \qquad (1)$$

where L_b and L_i are the bonded area length and the bond interface length, respectively.

For each dielectric embedded with both the higher and lower parameter combination, two samples were cross-sectioned and microscopically investigated. Each sample was cut into

front middle and rear sections (Fig. 5) which were mounted in epoxy resin and then gradually grinded and polished to 0.05 µm finish. An Olympus BX60M optical microscope with a ×100 magnification lens was used to take images for LWD calculation. For each mounted section, six images of weld interface were taken from both sides of the embedded dielectric.
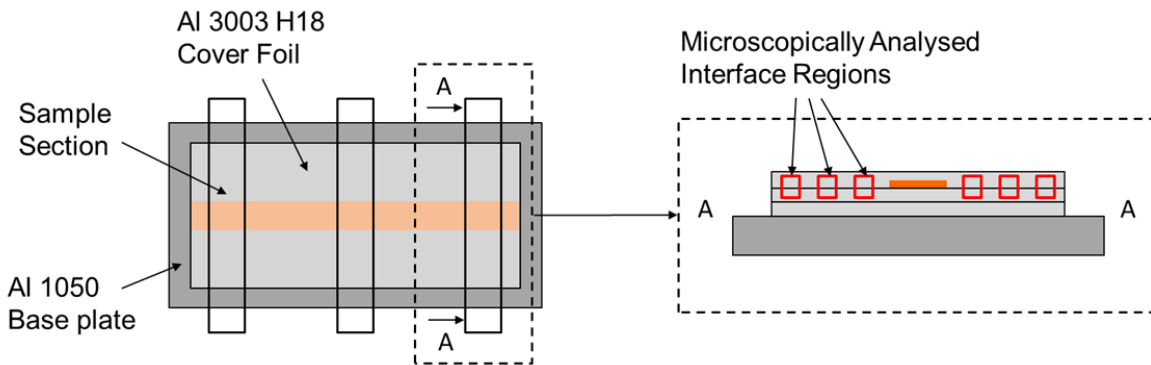

Fig. 5: Method of sample sectioning and microscopic analysis to determine the linear weld density via optical microscopy.

3. Results

3.1 Mechanical Peel Testing and Vickers Hardness

The peel testing was performed as described in section 2.2. The average maximum peeling load for the three dielectric films embedded with the two combinations of UAM parameters were plotted in Fig. 6.
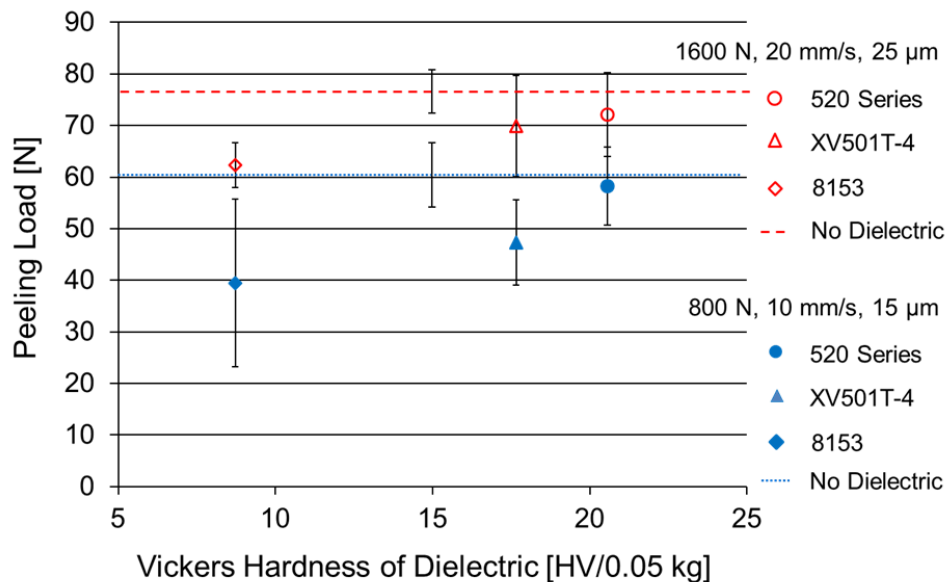

Fig. 6: The average maximum peeling loads for three different hardness dielectric films embedded with two combinations of UAM parameters.

For each combination of UAM process parameters, the peeling load increased with the dielectric hardness. For each dielectric, the samples encased with higher UAM process energy (1600 N force, 20 mm/s speed, and 25 µm) exhibited larger peeling load than those made by lower UAM process energy (800 N force, 10 mm/s speed, and 15 µm). Compared with the samples embedded without dielectric film that were used to characterize the mechanical strength of aluminium matrices, the peeling load of the harder dielectric such as 520 Series reduced slightly by around 8 %, whereas for the softer dielectric (8153) a dramatic reduction (more than 20 %) was observed. Moreover, there was a significant standard deviation (± 16 N) on the peeling load of 8153 encased by lower UAM process energy.

3.2 Optical Microscopy and Vickers Hardness

The LWD was measured and then calculated for each dielectric via the microscopic analysis of sample cross-sections. The average LWDs are demonstrated graphically in Fig. 7.

The general tendency was that higher UAM processing energy and a harder dielectric resulted in a higher average LWD. It is noticeable that average LWD of 8153 embedded using lower UAM processing energy also showed a large deviation (around 27 % in percentage). Both of these were in accordance with the peeling load results.
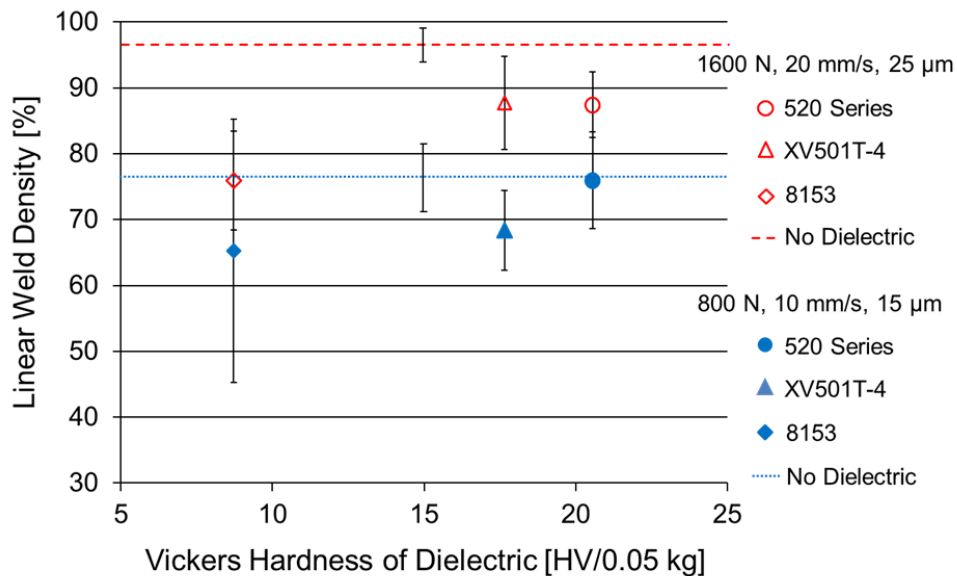

Fig. 7. Linear weld density for three different hardness dielectric films embedded with two combinations of UAM parameters.

3.3 Discussion

The mechanical strength of UAM samples with embedded dielectric was enhanced following the increase of dielectric hardness (Fig. 6); this result correlates with increased LWDs, shown in Fig. 7, which also increased with dielectric hardness. This phenomenon was likely caused by the deformation of dielectric film during UAM embedding. Hard dielectric had high

resistance to deformation when the UAM load was applied, so the shape of the dielectric film could be maintained. On the contrary, soft dielectric as in 8153 was found to be squashed and squeezed into the Al-Al weld area (Fig. 8). With large UAM embedding energy 8153 was deformed and squeezed uniformly along the welding direction. This resulted in a dramatic reduction of LWD in Fig. 7. Due to sufficient UAM processing energy and the regular spread of dielectric film, the standard deviations of LWD was less than ± 7 %. However, in the case of low UAM energy, a significant deviation of LWD occurred as the UAM processing energy was not sufficient to suppress the Al cover layer to adapt the irregular dielectric material expansion. In both cases, the squash of dielectric layer caused the mechanical strength degradation of the UAM embedded structure.
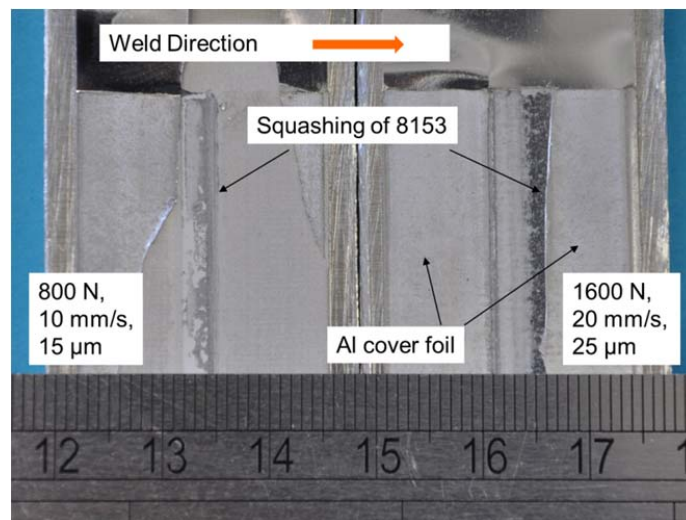

Fig. 8. The squashing of 8153 into the Al-Al weld area due to UAM prcessing.

By observing all the samples after peel testing, no bonding was found in the interface between the dielectric films and the Al cover foils, which indicated that there was no melting of dielectric material during UAM embedding.

4. Conclusions

This work successfully deposited via screen printing and embedded via UAM a range of dielectric films thus demonstrating their compatibility with the UAM process. This result makes it clear that the direct embedding of screen printed electronic materials within solid state additively manufactured metal matrices is feasible.

Peel testing and cross-sectional microscopy showed that the mechanical strength of dielectric containing UAM samples increased with the dielectric materials hardness. The greater deformation of the softer dielectric materials caused by UAM processing was found to be the reason for the reduction in mechanical strength. For each dielectric, it was also observed that mechanical strength of the samples was improved when using higher UAM processing energy.

In the near future, an electrical conductive structure will be deposited and encapsulated within the dielectric film before UAM encapsulation. This work is expected to then lead onto the

creation of UAM devices with integrated electrical components thus realising a multifunctional metal matrix composite.

Acknowledgement

References

[1]   White, Dawn R. "Ultrasonic consolidation of aluminum tooling." Advanced materials & processes 161, no. 1 (2003): 64-65.

[2]   Kong, Choon Yen, and Rupert C. Soar. "Method for embedding optical fibers in an aluminum matrix by ultrasonic consolidation." Applied optics 44, no. 30 (2005): 6325-6333.

[3]   Siggard, Erik J., Anand S. Madhusoodanan, Brent Stucker, and Brandon Eames. "Structurally embedded electrical systems using ultrasonic consolidation (UC)." In Proceedings of the 17th Solid Freeform Fabrication Symposium, pp. 14-16, 2006.

[4]   Robinson, Christopher J., Brent Stucker, Amit J. Lopes, Ryan B. Wicker, and Jeremy A. Palmer. "Integration of direct-write (DW) and ultrasonic consolidation (UC) technologies to create advanced structures with embedded electrical circuitry." In Proceedings of the 17th Annual Solid Freeform Fabrication Symposium, pp. 60-69, 2006.

[5]   Janaki Ram, G. D., Y. Yang, and B. E. Stucker. "Effect of process parameters on bond formation during ultrasonic consolidation of aluminum alloy 3003." Journal of Manufacturing Systems 25, no. 3 (2006): 221-238.

[6]   Kong, C. Y., R. C. Soar, and P. M. Dickens. "Optimum process parameters for ultrasonic consolidation of 3003 aluminium." Journal of materials processing technology 146, no. 2 (2004): 181-187.

[7]   Kulakov, M., and H. J. Rack. "Control of 3003-H18 aluminum ultrasonic consolidation." Journal of Engineering Materials and Technology 131, no. 2 (2009): 021006.

[8]   DuPont Company, "DuPont™ LuxPrint® 8153 electroluminescent material." Technical Data, 2009.

[9]   Technic company, "520 serials thermal 2 pack solder resists." Technical Data, 2008.

[10]   SunChemical Company, "ImagecureSMART® XV501T-4 Screen." Technical Data, 2011.